Tracking #: 2006-07713 3rd revision

Classification Major category: Biological Science, Minor category: Neuroscience

Separate oscillating cell groups in mouse suprachiasmatic nucleus couple photoperiodically to the onset and end of daily activity

Natsuko Inagaki, Sato Honma*, Daisuke Ono, Yusuke Tanahashi and Ken-ichi Honma

Department of Physiology, Hokkaido University Graduate School of Medicine, Sapporo 060-8638, Japan

***Corresponding author:** Sato Honma, M.D. Ph.D.

Department of Physiology, Hokkaido University Graduate School of Medicine, North 15, West 7, Kita-ku, Sapporo 060-8638, Japan

Phone:+81-11-706-6058, Fax:+81-11-706-7871

E-mail: sathonma@med.hokudai.ac.jp

Manuscript information: Number of text pages, 20. Number of table, 1. Number of figures, 5. (Number of color figures, 5) Number of supporting figure, 3.

Number of words in abstract, 245. Total number of characters in the paper including space, 34345

Author contributions: N.I., S.H. and K.H. contributed equally to this work.

Abbreviations: AVP, arginine vasopressin; E, evening oscillator; M, Morning oscillator; DD, constant darkness; LD**,** light and dark cycle; LL; constant light, ψ: phase

angle difference; SCN, suprachiasmatic nucleus; VIP, vasoactive intestinal peptide.

The pattern of circadian behavioral rhythms is photoperiod-dependent, highlighted by the conservation of a phase-relation between the behavioral rhythm and photoperiod. A model of two separate but mutually coupled circadian oscillators has been proposed to explain photoperiodic responses of behavioral rhythm in nocturnal rodents: an evening (E) oscillator which drives the activity onset and entrains to dusk, and a morning (M) oscillator which drives the end of activity and entrains to dawn. Continuous measurement of circadian rhythms in clock gene *Per1* expression by a bioluminescence reporter enabled us to identify the separate oscillating cell groups in the mouse suprachiasmatic nucleus (SCN), which composed circadian oscillations of different phases and responded to photoperiods differentially. The circadian oscillation in the posterior SCN was phase-locked to the end of activity under three photoperiods examined. On the other hand, the oscillation in the anterior SCN was phase-locked to the onset of activity, but showed a bimodal pattern under a long photoperiod (LD 18:6). The bimodality in the anterior SCN reflected two circadian oscillatory cell groups of early and late phases. The anterior oscillation was unimodal under intermediate (LD12:12) and short (LD6:18) photoperiods, which was always phase-lagged behind the posterior oscillation when the late phase in LD18:6 was taken. The phase difference was largest in LD18:6 and smallest in LD6:18. These findings indicate that three oscillating cell groups in the SCN constitute regionally specific circadian oscillations, and at least two of them are involved in photoperiodic response of behavioral rhythm.

Adaptation to seasonal changes in environment is critical to the survival of many organisms. Photoperiodic time measurement by the circadian clock is one of the strategies by which they conserve the phase-relation between behavioral events such as the activity onset and dawn or dusk[1]. A dramatic change induced by photoperiod is in the length of an activity band, the duration of activity in behavioral rhythms. Nocturnal rodents such as rats and mice exhibit compressed activity bands in long photoperiods and decompressed bands in short photoperiods. A long-standing hypothesis for the photoperiodic time measurement assumes two separate but mutually coupled circadian oscillators which drive the activity onset and end of activity, respectively, and which respond to dawn and dusk differentially. Therefore, their phase-relationship encodes day lengths and changes the length of an activity band[1].

The circadian clock in mammals is located in the suprachiasmatic nucleus (SCN) of the hypothalamus; it entrains to the light-dark cycle and determines the phases of overt circadian rhythms in behavior and physiology[2]. Over the last decade, our understanding of the circadian clock in the SCN has advanced tremendously[3-5]. The SCN consists of a number of oscillating cells in the circadian domain, which are independent but coupled with each other to produce coherent SCN output rhythms[4-8]. The intracellular molecular machinery of circadian oscillation consists of interlocked transcriptional and translational auto-feedback loops, in which at least 6 clock genes are involved[3]. *Clock* and *Bmal1* are positive elements of the feedback loop, and *Per1, Per2, Cry1* and *Cry2* are negative elements.

There is substantial evidence that the SCN contains at least two independent sub-oscillators. Circadian rhythms in two major neuropeptides in the SCN, arginine vasopressin (AVP) and vasoactive intestinal peptide (VIP), free-ran *in vitro* with

different periods and showed internal desynchronization[9]. More recently, two distinct peaks of electrophysiological activity in the cultured SCN were observed in the Syrian hamster[10,11], and the peaks responded differentially to photoperiods[10]. In addition, circadian rhythms in clock gene expression and their protein products were reported to change in different photoperiods[12-17]. Generally, the interval of high *Per1* and *Per2* expression is extended in long photoperiods, whereas the rhythm amplitudes are increased in short photoperiods. Johnston and his colleagues[18,19] observed differential phasing of clock gene expression rhythms in the rostral and caudal regions of the hamster SCN, and proposed a model in which the E oscillator is located in the rostral and the M oscillator in the caudal SCN[19].

Transgenic mice carrying a luciferase reporter gene enable us to search for the E and M oscillators, or even the E and M oscillating cells in the SCN. In the present study, we tried to separate oscillating cell populations which respond differentially to photoperiod using transgenic mice with a *Per1*-luciferase reporter system. We found oscillating cell groups in the SCN, which were phase-locked separately to the activity onset and end of activity, and whose phase-relations were changed by photoperiod.

Results

Behavioral rhythms in different photoperiods

Photoperiodic responses of spontaneous activity rhythms were examined in the transgenic mice carrying a *Per1*-luciferase reporter gene (*Per1*-luc) initially kept in 12h light and 12h darkness (LD12:12) (Fig 1A). Nocturnal activities of these mice were bimodal, showing the clear activity onset and end of activity in constant darkness (DD) as well as in LD. In steady state entrainment, the length of activity band, an interval

between the activity onset and the end of activity, was decreased (compression) by 5.26 h when the animals were transferred to LD18:6, and increased (decompression) by 1.49h when transferred to LD 6:18 (Table 1, Fig.1B). The compressed activity band in LD18:6 was decompressed again when released into DD with a transient period of about 2 weeks (Supporting Fig.1). The phase angle difference between the activity onset and light-off (ψ_{onset}) was basically unchanged in LD18:6, but became slightly but significantly more negative ($p<0.01$) by -0.99h in LD6:18. On the other hand, the phase angle difference between the end of activity and light-on (ψ_{end}) were significantly changed ($p<0.01$) in LD18:6 as well as LD 6:18 by -0.96h and by 3.53h , respectively (Fig.1B).

***Per1*-luc expression rhythms in the SCN slices**

Circadian rhythms in *Per1-luc* were measured separately in the anterior and posterior SCN slices (Supporting Fig.2A,B). Robust circadian rhythms in *Per1-luc* activity were detected in all preparations, except for the anterior SCN in LD18:6, and the circadian peak phases on the first day of culture were located in the subjective day (Fig. 2A). The circadian peak on the first cycle in the anterior and posterior SCN were located at local time 13.69±0.98h (mean±SD, n=10) and 11.44±0.68h (n=9) in LD12:12, which shifted to 12.20±0.57h (n=9) and 10.45±1.11h in LD6:18 (n=10), respectively. In the anterior SCN obtained from mice in LD18:6, the two antiphasic peaks were detected in the first few days of culture, which were located at the rising phase (6.75±0.69h) and falling phase (16.66±0.95h) (n=10) of the posterior peak. The bimodal pattern became evident in the detrended curves (Fig.2B). The posterior peak was located at 8.02±1.75h (n=8) on the first day. In 9 out of 10 anterior SCN slices from LD18:6, the two peaks merged into a single circadian peak on the course of culture

(Fig.2C uppermost). Distribution of the posterior peaks was significantly wider in LD 18:6 than in LD12:12 and LD6:18 ($p<0.01$ and $P<0.05$, respectively).

The phase relations were examined between the first day peaks and photoperiods as well as behavioral rhythms of mice from which the SCNs were sampled (Fig.3A). The two peaks in the anterior SCN from LD18:6 were tentatively termed as A_E and A_M, where A_E was closer to the light-off and A_M to the light-on. Neither the anterior nor the posterior peaks from different photoperiods showed a consistent phase-relation with the light-on or light-off. On the other hand, stable phase relations were observed between the anterior peaks (A_E) and activity onset ($\psi_{Per1\text{-onset}}$), and between the posterior peaks and end of activity ($\psi_{Per1\text{-end}}$) in three photoperiods examined (Fig.3B). The $\psi_{Per1\text{-onset}}$ was kept at approximately 4.3 hours (4.70±1.13h in LD18:6; 4.59±0.86h in LD12:12; 3.63±0.45h in LD6:18) for the anterior perks and the $\psi_{Per1\text{-end}}$ was kept at about -4.4 hours (-3.63±1.59h in LD18:6; -4.80±0.80h in LD12:12; -4.70±1.12h in LD6:18) for the posterior peak. The correlations between the *Per1* peak and 4 phase markers (activity-onset, end of activity, light-on and light-off) were calculated. The anterior peak (A_E) was correlated most strongly with the activity onset ($r=0.904$), and the posterior peak with the end of activity ($r=0.713$).

The posterior peak phase-led the anterior (A_E) peak significantly. The phase difference was largest in LD18:6 (8.66±1.78h), intermediate in LD12:12 (2.08±0.98h) and smallest in LD6:18 (1.55±0.87h) on day1.

***Per1*-luc expression rhythms in the SCN cells**

To clarify the nature of two peaks in the anterior SCN slices from mice in LD18:6 and to identify the localizations of anterior and posterior peaks in the SCN, *Per1*-luc expression was measured in individual SCN cells for more than three circadian

cycles using bioluminescent cell imaging (Fig.4,5A). Regardless of the anterior or posterior SCN, almost all cells which exhibited bioluminescence at detectable levels showed circadian rhythms in *Per1*-luc expression with a single peak. The intensity of bioluminescence was slightly and non-systematically different between the right and left SCN, but no evidence was detected to suggest the lateralization of the circadian peak.

Circadian peaks in individual SCN cells detected on the first culture day were plotted against the local time (Fig.5B). In LD18:6, the temporal distribution was bimodal in the anterior SCN, whereas it was unimodal in the posterior. Bimodal patterns were detected in the peak distribution in all 3 SCN slices examined. The distribution of the early group peaked at 7.77±1.67 h, while the late group at 14.54±1.42 h, respectively (Supporting Fig.3). The early group corresponded to A_M and the late one to A_E in the SCN slices. Number of A_M and A_E cells were almost equal in three slices examined, and out of 292 cells in total, 142 belonged to the A_M cells and the 142, to A_E cells. Eight cells (2.7%) between A_M and A_E at 11:00h could not be classified. The distribution peak in the posterior SCN cells was located at 12.35±2.83h (n=152). By contrast, the distribution of circadian peaks in individual cells was unimodal in LD12:12 and LD6:18 in both the anterior and posterior SCN, with peaks at around the middle of subjective day (Supporting Fig.3). When the range of distribution was defined as SD, the distributions in the anterior SCN were significantly wider than those in the respective posteriors ($p<0.01$). The range of distribution in the posterior SCN was significantly narrower in LD 12:12 and LD 6:18 than in LD18:6 ($p<0.01$ and $p<0.05$, respectively).

Figure 5C illustrates spatial distribution of individual cells in the anterior SCN from LD18:6, which belong to either the A_M or A_E cells. The A_M and A_E cells were

widely distributed in the anterior SCN and intermixed.

Discussion

Continuous monitoring of *Per1* expression activity in the cultured SCN cells revealed that at least three different oscillating cell populations exist in the mouse SCN; two in the anterior and one in the posterior SCN. They appear to form functional cell networks with humoral or neural communications, and respond differentially to photoperiod. Changes in the 24 h profiles of bioluminescence rhythm in the SCN slice under different photoperiods are mostly the reflection of changes in the phase-relation, not the waveform, of individual oscillating cells (Fig. 5), as recently suggested by electrophysiology[20] and simulation studies[21].

The one of two oscillating cell populations (A_E cells) in the anterior SCN was correlated most strongly with the activity onset, while the cell population in the posterior SCN was correlated most strongly with the end of activity (Fig.3B). The length of an activity band, which reflects the phase relation between the activity onset and end of activity, depended on photoperiod (Fig1), and increased (decompressed) in a shorter photoperiod (LD6:18) and decreased (compressed) in a longer photoperiod (LD18:6). In parallel with compression and decompression of an activity band, the phase relation between the anterior (A_E) and posterior oscillations was changed in different photoperiods. The posterior oscillation phase-led the anterior in three photoperiods examined (Fig.3A). Therefore, the cell populations in the anterior and posterior SCN are likely to correspond to the E and M oscillators, respectively. The findings in part support a model advanced recently by Johnston et al[19]. In their model, however, the circadian peaks in the SCN are correlated with photoperiod, whereas our

results indicate strong correlations between the circadian oscillations in the SCN and behavioral rhythms. In addition, our results demonstrated the third oscillation in the anterior SCN. The circadian system in the SCN for photoperiodic responses seems to be more complex.

The A_M cell population in the anterior SCN became evident in a longer photoperiod (LD18:6), especially in the first several days of culture. Eventually, their oscillation peaks merged with the peaks of A_E oscillation, suggesting that they are not direct responses to light but expressions of endogenous oscillation, and there are coupling mechanisms between them. The numbers of cells categorized to the A_E or A_M population were nearly the same, and both groups of cells seem to spatially distribute rather diffusely and are intermixed (Fig.5C). The role of A_M oscillation was unidentified, but seems to be related to photoperiodic time measurement. The A_E oscillation in the anterior SCN and the oscillation in the posterior SCN are closely related with behavioral rhythms, but it is not known whether they are directly phase-locked by photoperiod or through other mechanisms. In LD18:6, the circadian peak of the posterior cell population was located in between those of the A_E and A_M cell populations. In shorter photoperiods, the A_M cell population seemed to disappear, but the ranges of peak distribution were still wider in the anterior SCN than in the posterior (Fig.5B). The A_M oscillation may have some roles in determining the phases of the A_E oscillation.

We reported a dissociation of circadian rhythms in AVP and VIP secretion during the prolonged culture of rat SCN[9,22], and suggested that AVP and VIP secretion was regulated by separate circadian oscillators in the SCN. Using green fluorescent proteins as a reporter, Quitero et al[8] reported differentially-phased three *Per1* expressing

cell groups and suggested their role in photoperiodic responses. Jagota et al showed two distinct peaks of electrophysiological activity in the horizontally sectioned SCN culture in hamsters[10] but not in rats and mice[11], which responded differentially to photoperiods. In addition, the circadian rhythms in *Per1* and *Per2* expression were reported to change in different photoperiods[12-19,23]. The duration of gene expression was extended in long photoperiods, whereas the rhythm amplitudes were increased in short photoperiods, suggesting that the mutual coupling of individual cell oscillations was altered by photoperiods.

The E and M oscillators have been proposed as the mechanism of rhythm splitting in hamsters under prolonged constant light (LL)[1]. Previously, the circadian rhythm in clock gene expression was demonstrated to be antiphasic in the right and left SCNs from hamsters exhibited behavioral splitting in LL[24]. More recently, two antiphase oscillating subregions were reported in each side of the SCN of split hamsters[25]. However, it is not known whether the E and M oscillators for the photoperiodic responses are identical to those for behavioral splitting or not, because a unilateral SCN has a redundancy for behavioral splitting as demonstrated by SCN transplants[26] and unilateral SCN lesion[27].

Per1 and *Cry1* have been hypothesized to represent the components of M oscillator, and *Per2* and *Cry2* the components of E oscillator[28]. The hypothesis is based on differential responses to light in the respective mutant animals[14, 28]. From the present studies, the photoperiodic response of behavioral rhythms in nocturnal rodents is explained without assuming differential roles of *Per1* and *Per2*, although the possibility remains that a single SCN cell contains the coupled E and M oscillators, in which *Per1* and *Per2* compete for dominancy. Specific pacemaker cells may exist in

the SCN which drive other cells to constitute separate oscillations as reported recently in *Drosophila* in which specific pacemaker cell groups[29], one processes the light information to convey into circadian networks, while the other dominates in activity output[30]. Alternatively, specific cell communication may enable coherent oscillations of different nature.

In conclusion, the present findings indicate that three distinct cellular oscillations in the SCN change their phases in response to the photoperiod and at least two of them are strongly coupled to the onset and end of activity, separately, in mice.

Methods

Per1-luc transgenic mice

We developed *mPer1-luc* transgenic mice with a firefly luciferase reporter on a C57BL/6J background. A 6.7-kb region upstream of the transcription-translation codon of the *mPer1* gene was linked to a firefly luciferase cDNA (a generous gift of Dr.Tei[31]) to make the transgene. *Per1-luc* mice were born and reared in our animal quarters where environmental conditions were controlled (12 h light and 12 h dark, lights: 06:00-18:00 h). Animals were cared for according to the Guidelines for the Care and Use of Laboratory Animals in Hokkaido University Graduate School of Medicine.

Measurement of behavioral rhythms

Male *Per1-luc* mice of 5~8 week old (n=18) were housed individually in a cage placed in a light-tight chamber. Spontaneous locomotor activity was monitored by thermal sensors[32]. Photoperiod was changed by phase-delaying the light-off and phase–advancing the light-on by 3h each for LD18:6, and by phase-advancing the

light-off and phase–delaying the light-on by 3h each for LD6:18. The onset and end of nocturnal activity were determined using behavioral rhythms of the last 5 days in each of three photoperiods (LD12:12, LD18:6, and LD6:18) by visual inspection (Clock Lab, Actimetrics).

SCN culturing and bioluminescent measurement

After monitoring behavioral rhythms for 3 weeks in the respective photoperiod, mice (n=30) were decapitated following cervical dislocation and brains were rapidly removed between 11:00 and 15:00, local time. Using a microslicer (D.S.K: DTK-1000), two successive coronal brain slices of 300μm thick containing the anterior and posterior regions of each SCN were cut for bioluminescence measurement with photomultiplier tubes (PMT). Bilateral SCNs with optic chiasms were trimmed to ≈3×3 mm square in ice cold HANKS' balanced salt solution and placed on a culture membrane (Millicell-CM, Millipore Corporations: pore size 0.4μm) in a 35mm Petri dish. SCN slices were cultured in air at 37°C with 130μl Dulbecco's modified Eagle's medium (DMEM) (Invitrogen Corporation) supplemented with 10mM HEPES, 2.74mM $NaHCO_3$, 0.1 mM D-Luciferin K salt (DOJINDO) and serum-free growth supplements described elsewhere[33]. Bioluminescence from each SCN slice was measured by a microplate luminometer equipped with PMTs (Lumicycle, Actimetrics), for 1 min at 9 min intervals for 5 successive days.

For single cell analysis, 5 successive coronal slices of 100μm thick were prepared through the rostrocaudal extent of the SCN from 9 mice. The 2nd and 4th slices were chosen as anterior and posterior SCN slices, respectively. Slices were cultured at 37˚C in a mini-incubator (Phoenix, IMP, Tokyo) installed on the stage of an inverted microscope (Leica, DM IRB). Bioluminescence from SCN cells was

measured with a high-sensitive cryogenic CCD camera (ORCA-II ER, HAMAMATSU photonics) mounted at the bottom port of the microscope with a camera adaptor of 0.6x. Bioluminescence was measured every hour with a 59 min exposure and a 1 min interval for data transfer for 3 consecutive days. CCD imaging of an SCN slice was performed using 10x objective lens (Leica, NA) at 4 x 4 binning of the 1344 (Horizontal) x 1024 (Vertical) pixel array. The final pixel number and pixel size of an image for detection were 336 x 256 and 4.3 μm × 4.3 μm, respectively.

Double-labeling immunohistochemistry.

SCN slices were immunohistochemically labeled using anti-mouse AVP monoclonal antibody (generous gift of Dr.Gainer[34]) and anti-rabbit VIP polyclonal antibody (Peptide Institute, Osaka, Japan).

Data and statistical analyses

Circadian rhythms in *Per1-luc* measured by Lumicycle were smoothed by a 5 point moving average method, and the peak phases were calculated after detrending bioluminescent levels using first order regression for each cycle. To analyze circadian rhythms in single cells, individual cells were identified by inspection and the region of interest (ROI) was defined to cover most of the cell bodies. Bioluminescence of a given ROI was expressed with an averaged intensity per pixel by Aquacosmos (HAMAMATSU photonics). The circadian peak of bioluminescent rhythms was defined as the midpoint of two succeeding troughs in each cycle. For the analyses of phase-relation between circadian rhythms in *Per1-luc* activity and behavioral rhythms, 5 day records of behavioral rhythms immediately before the brain sampling were used.

Statistical significance of differences in parameters among three photoperiods was evaluated with one-way ANOVA and a post-hoc Tukey-Kramer test. Unpaired

student's t-test was used for group comparisons. Paired student's t-test was used for comparison of parameters of behavioral rhythms in different photoperiods. Differences in the peak distribution among photoperiods were evaluated by F-test following Bartlett test. Linear regression was obtained between the *Per1* peak of SCN slice and one of 4 phase markers; activity-onset, activity-end, light-on and light-off.

Note: A related report by van der Leest et al. (*Curr. Biol.***17**: 468-473, 2007) has been published during the revision of the manuscript.

References

1. Pittendrigh, C. S., & Daan, S. A functional analysis of circadian pacemakers in nocturnal rodents. V. Pacemaker structure : a clock for all seasons. (1976) *J. Comp. Physiol. A.* **106**, 333-355.
2. Klein, D. G.., Moore, R. Y., & Reppert, S. M. (1991) Suprachiasmatic nucleus; the mind's clock. *Oxford University Press, Inc*. New York.
3. Reppert, S. M., & Weaver, D. R. Coordination of circadian timing in mammals. (2002) *Nature* **418**, 935-941.
4. Yamaguchi, S., Isejima, H., Matsuo, T., Okura, R., Yagita, K., Kobayashi, M., & Okamura, H. Synchronization of cellular clocks in the suprachiasmatic nucleus. (2003) *Science* **302,** 1408-1412.
5. Antle, M. C., & Silver, R. Orchestrating time: arrangements of the brain circadian clock. (2005) *Trends Neurosci*. **28**, 145-151.
6. Welsh, D. K., Logothetis, D. E., Meister, M., & Reppert, S. M. Individual neurons dissociated from rat suprachiasmatic nucleus express independently phased circadian firing rhythms. (1995) *Neuron* **14**, 697-706.
7. Honma, S., Shirakawa, T., Katsuno, Y., Namihira, M., & Honma., K. Circadian periods of single suprachiasmatic neurons in rats. (1998) *Neurosci. Lett.* **250**, 157-160.
8. Quintero, J. E., Kuhlman, S. J., and McMahon, D. G. The biological clock nucleus: a multiphasic oscillator network regulated by light (2003) *J. Neurosc*i. **23**: 8070-8076.
9. Shinohara, K., Honma, S., Katsuno, Y. Abe, H., & Honma, K. Two distinct oscillators in the rat suprachiasmatic nucleus in vitro. (1995) *Proc. Natl. Acad. Sci. USA.* **92**, 7396-7400.

10. Jagota, A., de la Iglesia, H. O., & Schwartz, W. J. Morning and evening circadian oscillations in the suprachiasmatic nucleus in vitro. (2000) *Nature Neurosci*. **3**, 372-376.

11. Burgoon, P. W., Lindberg, P. T., & Gillette, M. U. Different patterns of circadian oscillation in the suprachiasmatic nucleus of hamster, mouse and rat. (2004) *J. Comp. Physiol. A.* **190**, 167-171.

12. Messager,S., Ross, A.W., Barrett, P., & Morgan, P.J. Decoding photoperiodic time through *Per1* and ICER gene amplitude. (1999) *Proc.Natl.Acd.Sci.USA* **96**, 9938-9943.

13. Nuesslein-Hildesheim, B., O'Brien, J. A., Ebling, F. J. P., Maywood, E. S., & Hastings, M. H. The circadian cycle of mPER clock gene products in the suprachiasmatic nucleus of the Syberian hamster encodes both daily and seasonal time.(2000) *Eur.J.Neurosci.***12**:2856-2864.

14. Steinlechner, S., Jacobmeier, B., Scherbarth, F., Dernbach, H., Kruse, F., & Albrecht, U. Robust circadian rhythmicity of *Per1* and *Per2* mutant mice in constant light, and dynamics of *Per1* and *Per2* gene expression under long and short photoperiods. (2002) *J. Biol. Rhythms* **17**, 202-209.

15. Carr, A-J. F., Johnston, J.D., Semikhodskii, A.G., Nolan, T., Cagampang, F. R., Stirland, J. A., & Loudon, A. S. Photoperiod differentially regulates circadian oscillators in central and peripheral tissues of the Syrian hamster. (2003) *Curr. Biol.* **13**, 1543-1548.

16. Sumova, A. Jac, M., Sladek. M., Sauman, I., & Illnerova, H. Clock gene daily profiles and their phase relationship in the rat suprachiasmatic nucleus are affected by photoperiod. (2003) *J. Biol. Rhythms* **18**, 134-144.

17. Johnston, J. D., Ebling, F. J. P. & Hazlerigg, D. G. Photoperiod regulates multiple gene expression in the suprachiasmatic nuclei and pars tuberalis of the Siberian hamster (Phodopus sungorus). (2005) *Eur. J. Neurosci*. **21**, 2967-2974.

18. Hazlerigg, D. G., Ebling, F. J. P., & Johnston, J. D. Photoperiod differentially regulates gene expression rhythms in the rostral and caudal SCN. (2005) *Curr. Biol*. **15**, 449-450.

19. Johnston, J. D. Measuring seasonal time within the circadian system: regulation of the suprachiasmatic nuclei by photoperiod. (2005) *J. Neuroendocrinology* **17**, 459-465.

20. Schaap, J., Albus, H. van der Leest, H.T. Eilers, P. H. C. Détári, L., & Meijer, J. H. Heterogeneity of rhythmic suprachiasmatic nucleus neurons: Implications for circadian waveform and photoperiodic encoding. (2003) *Proc. Natl. Acad. Sci. U.S.A.* **100**:15994-15999.

21. Rohling, J. Wolters, L., & Meijer, J. H. Simulation of day-length encoding in the SCN: from single-cell to tissue level organization. (2006) *J.Biol.Rhythm* **21**:301-313.

22. Nakamura**,** W., Honma, S.**,** Shirakawa, T., Oguchi, H., & Honma, K. Regional pacemakers composed of multiple oscillator neurons in the rat suprachiasmatic nucleus. (2001) *Eur. J. Neurosci*. **14**, 666-674.

23. de la Iglesia, H. O., Meyer, J., & Schwartz, W. J. Using Per gene expression to search for photoperiodic oscillators in the hamster suprachiasmatic nucleus. (2004) *Mol. Brain Res*. **127**, 121-127.

24. de la Iglesia, H., Meyer, J., Carpino, A. Jr., & Schwartz, W. J. Antiphase oscillation of the left and right suprachiasmatic nuclei. (2000) *Science* **290**, 799-801.

25. Yan, L., Foley, N. C., Bobula, J. M., Kriegsfeld L. J., and Silver, R. Two antiphasic oscillations occur in each suprachiasmatic nucleus of behaviorally split hamsters. (2005) *J. Neurosci.* **25**:9017-9026.

26. Davis, F. C., & Viswanathan, N. The effect of transplanting one or two suprachiasmatic nuclei on the period of the restored rhythm. (1996) *J.Biol.Rhythms* **11**,291-301.

27. Davis, F. C., & Gorski, R.A. Unilateral lesions of the hamster suprachiasmatic nuclei: Evidence for redundant control of circadian rhythms. (1984) *J.Comp.Physiol. A* **154**, 221-232.

28. Daan, S., Albrecht, U., van der Horst, G.T., Illnerova, H., Roenneberg, T., Wehr, T.A., & Schwartz, W.J. Assembling a clock for all seasons: are there M and E oscillators in the genes? (2001) *J. Biol. Rhythms* **16**, 105-116.

29. Stoleru, D., Peng, Y., Nawathean, P., & Rosbash, M. A resetting signal between Drosophila pacemakers synchronizes morning and evening activity. (2005) *Nature* **438**, 238-242.

30. Stoleru, D., Nawathean, P., de la Paz Fernandez, M., Menet, J. S., Ceriani, M.F. & Rosbash, M. The *Drosophila* circadian neuronal network is a seasonal timer. (2007) *Cell* (in press)

31. Hida, A., Koike, N., Hirose, M., Hattori, M., Sakaki, Y., & Tei, H. The human and mouse *Period1* genes: five well-conserved E-boxes additively contribute to the enhancement of m*Per1* transcription. (2000) *Genomics* **65**, 224-233.

32. Honma, K., Honma, S., Shirakawa, T., & Hiroshige, T. Phase-setting of circadian locomotor rhythm of infant rats. (1987) *Am. J. Physiol.* **252**, 256–261.

33. Nakamura, W., Honma, S., Shirakawa, T., & Honma, K. Clock mutation lengthens

the circadian period without damping rhythms in individual SCN neurons. (2002) *Nature Neurosci*. **5**, 399-400.

34. Whitnall, M. H., Key, S., Ben-Barak, Y., Ozato, K., & Gainer, H.. Neurophysin in the hypothalamo-neurohypophysial system. 2. Immunocytochemical studies of the ontogeny of oxytocinergic and vasopressinergic neurons. (1985) *J Neurosci*. **5**, 98-109.

Acknowledgements We thank Dr. Hajime Tei for kindly donating the *Per1-luc* plasmid vector; Dr. Gainer for providing anti-mouse AVP monoclonal antibody. We are grateful to M. P. Butler for advice on the manuscript.

Legend of Figures

Figure 1. Circadian behavioral rhythms in different photoperiods

A, Representative double-plotted circadian rhythms in spontaneous locomotor activity of a mouse transferred to LD18:6 (left) and that to LD 6:18 (right) from LD 12:12. The dark phase is shaded in the right hand side of each actograph. Arrows indicate day of photoperiod transfer. **B**, Phase relations of activity rhythms to different photoperiods. Yellow bars indicate activity bands (mean±SD). Gray areas: dark phase.

Figure 2. *Per1-luc* activity rhythms of the anterior and posterior SCN slices in different photoperiods.

A, Representative rhythms of *Per1-luc* activity in the anterior (pink) and posterior (green) SCN in LD18:6 (upper panel), LD12:12 (middle panel), and LD6:18 (lower panel). Ordinate indicates strength of bioluminescence (relative light units, RLU). Abscissa indicates days in culture. Broken lines in the graph indicate 0:00 h. White bars on the abscissa, light phase on the day of slice preparation. Gray and black bars, the subjective day and night on the following days, respectively. **B**, Detrended waveforms of *Per1-luc* rhythms obtained by subtracting 12 h moving average values from original luminescence curves. **C,** Peak phases of *Per1-luc* rhythms from the anterior and posterior SCN slices are plotted against local time. Those from different mice are indicated with different colors. Ordinate: days in culture.

Figure 3. Correlation between behavior rhythms and *Per1-luc* rhythms in anterior and posterior SCN.

A, Phase relationships between the anterior and posterior peaks of the first two days in

different photoperiods. Symbols: peak phase (mean ± SD in hour, n=8 in LD18:6, n=9 in LD12:12 and n=8 in LD6:18). Gray areas, subjective night. *,**: $p<0.05$, 0.01 vs. posterior peak. Horizontal yellow bars: activity band (mean ± SD). +,++;$p<0.05$, 0.01 vs. ψ_{on} or ψ_{end} in LD12:12, and ##; $p<0.01$ ψ_{on} or ψ_{end} in LD18:6 vs. those in LD6:18. **B**, Phase differences (ψ) between the peak of *Per1-luc* expression rhythm and activity onset ($\psi_{Per1\text{-}onset}$, left panels), and between the peak and end of activity ($\psi_{Per1\text{-}end}$, right panels) in three photoperiods. Phase angle differences between the activity and bioluminescence rhythms were measured for each animal and averaged (mean ± SD). ** ; $p < 0.01$ vs. anterior SCN in LD12:12 ,+, ++ ; $p < 0.05$, 0.01 vs. posterior SCN in LD12:12.

Figure 4. CCD images of *Per1-luc* rhythms in single SCN cells.

A, Representative CCD images from the anterior and posterior SCN in different photoperiods. Single SCN cells indicated by colored circles correspond to cells with the number in the same color in Fig.4B. Scale bar, 100 μm. **B**, Serial demonstration of bioluminescence in a single cell at 1h intervals on day 1. In LD18:6 (upper), bioluminescence is strong either at the early or late subjective day in the anterior SCN, whereas it is strong at the middle of subjective day in the posterior. In LD6:18 (lower), individual rhythms are essentially the same between the anterior and posterior SCN with respect to circadian phase. Scale bar, 10 μm. A; anterior. P; posterior. L; left, R; right. A_M, A_E; Cells with morning and evening peaks for the anterior SCN in LD18:6, respectively. Gray and black horizontal bars, the subjective day and night, respectively.

Figure 5. Spatial and temporal distributions of circadian rhythms in *Per1-luc* from single SCN cells in different photoperiods.

A, 48h profiles of bioluminescence of individual cells in the anterior and posterior SCN slices obtained from a mouse in LD18:6 (upper panels), LD12:12 (middle panels) and LD6:18 (lower panels). **B**, Temporal distribution of individual circadian peaks (on day1) from the same SCNs indicated in **A**. Distribution peaks were expressed in each panel with the mean and SD of individual circadian peaks. See the supporting Fig.2 for the peak distribution of the total cells from 3 SCNs. **C**, Spatial distribution of cells with the morning (A_M, orange) and evening peaks (A_E, pink), in the anterior SCN under LD18:6 shown in **A**. Scale bar, 100 μm.

Table1. Parameters of behavioral rhythms in different photoperiods

Phase angle differences (ψ) were calculated between the activity onset and light-off (ψ_{onset}) , and between the end of activity and light-on (ψ_{end}). Paired student's t-test was used for comparing values of two different photoperiods.

Lighting (on - off)	Activity time (h) (Onset)	(End)	ψ (h) ψ_{onset}	ψ_{end}
LD12:12 (6-18 h)	12.61 ± 0.77 (18.16 ± 0.58)	(6.77 ± 0.34)	-0.16± 0.58	-0.77± 0.34
LD18:6 (3-21 h)	7.35 ±0.66** (21.38 ±0.34**)	(4.73 ± 0.44**)	-0.38 ± 0.34	-1.73 ± 0.44**

Lighting (on - off)	Activity time (h) (Onset)	(End)	ψ (h) ψ_{onset}	ψ_{end}
LD12:12 (6-18 h)	12.10 ± 0.47 (18.19 ± 0.22)	(6.29 ± 0.48)	-0.19 ± 0.22	-0.29 ± 0.48
LD6:18 (9-15 h)	13.59 ± 0.86** (16.18 ± 0.60**)	(5.76 ± 1.28)	-1.18 ± 0.60**	3.24 ± 1.28**

Values are mean ± SD (n=9) ** : $p < 0.01$ vs LD12:12

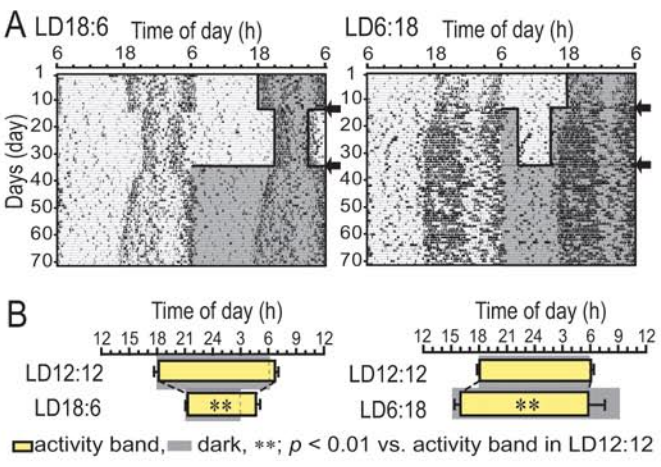
A
LD18:6
Time of day (h)
6 18 6 18 6
LD6:18
Time of day (h)
6 18 6 18 6
Days (day)
1 10 20 30 40 50 60 70
B
Time of day (h)
12 15 18 21 24 3 6 9 12
LD12:12
LD18:6
**
Time of day (h)
12 15 18 21 24 3 6 9 12
LD12:12
LD6:18
**
activity band, dark, **; p < 0.01 vs. activity band in LD12:12

Figure 1

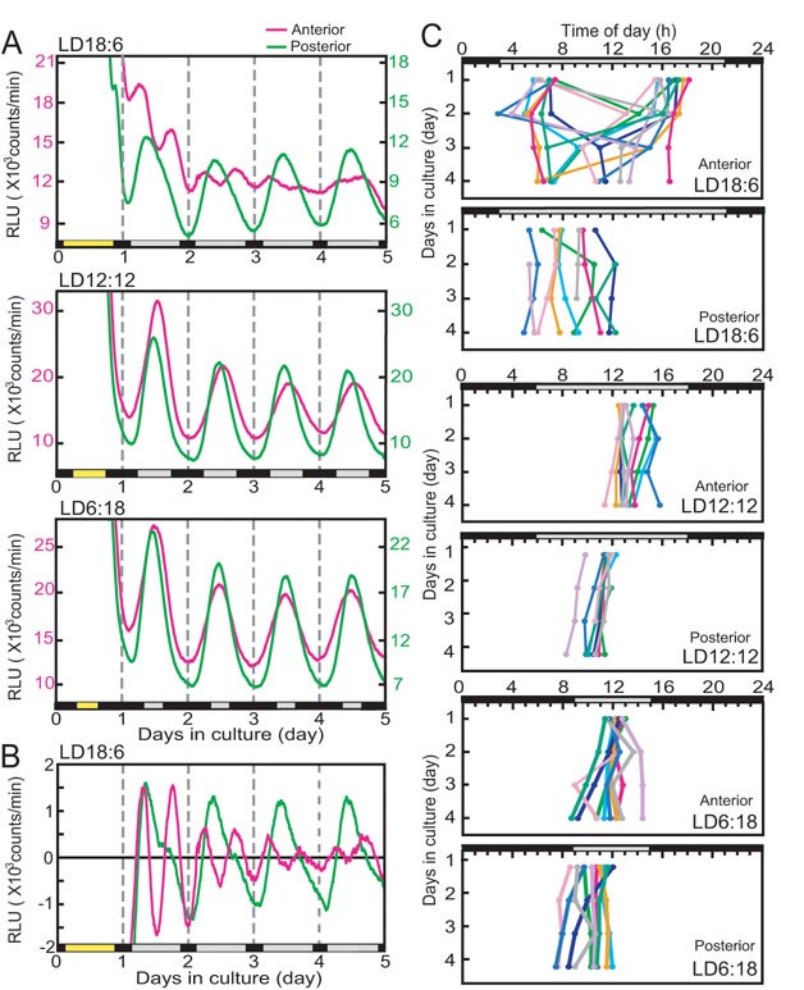
A
Anterior
Posterior
LD18:6
LD12:12
LD6:18
RLU (X10³counts/min)
Days in culture (day)
B
C
Time of day (h)
Days in culture (day)
Anterior
Posterior

Figure 2

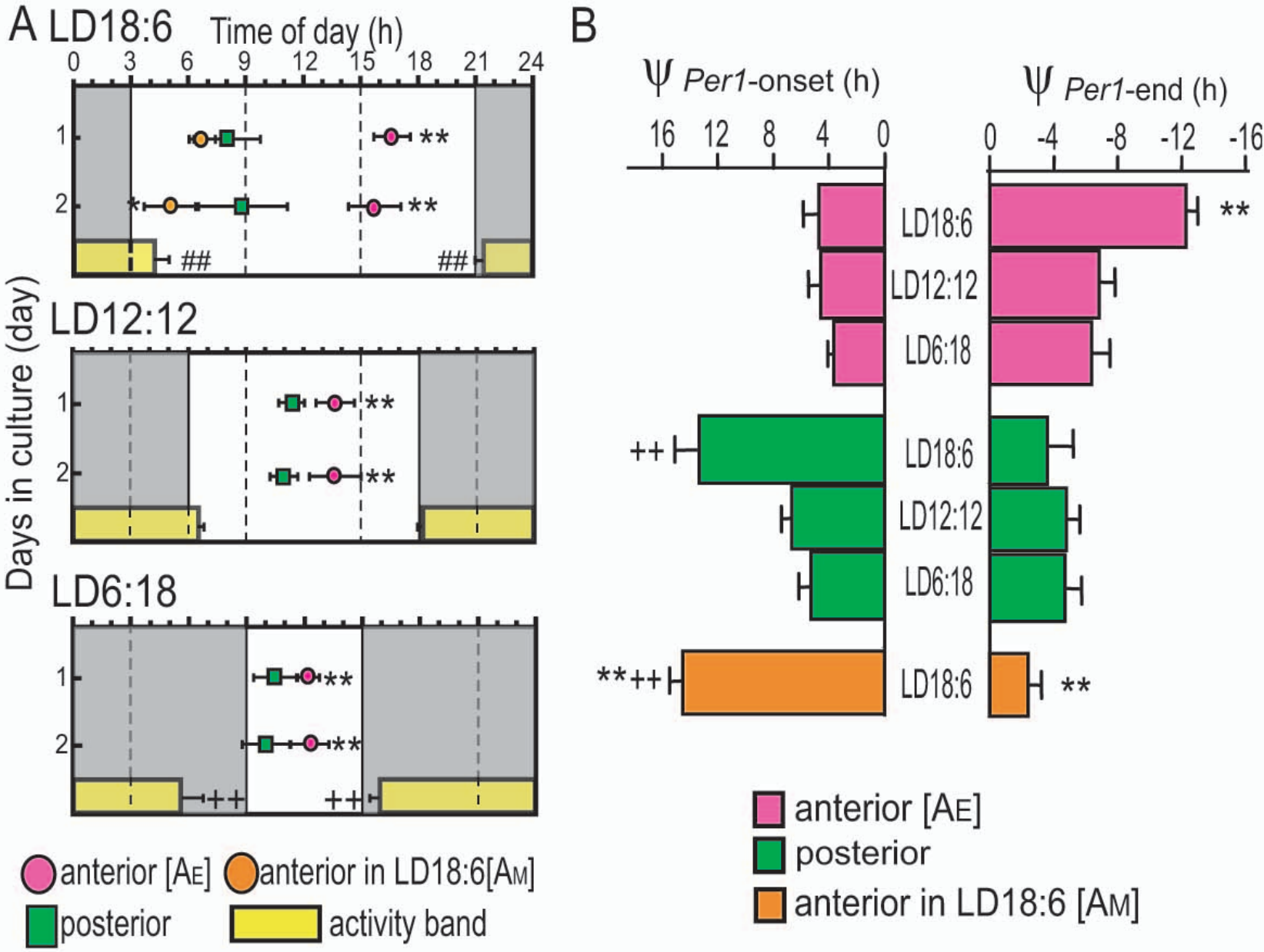
A LD18:6
Time of day (h)
0 3 6 9 12 15 18 21 24
1
2
**
*
**
##
##
LD12:12
1
2
**
**
LD6:18
1
2
**
**
++
++
Days in culture (day)
anterior [AE]
anterior in LD18:6[AM]
posterior
activity band
B
Ψ Per1-onset (h)
16 12 8 4 0
Ψ Per1-end (h)
0 -4 -8 -12 -16
LD18:6
LD12:12
LD6:18
**
++
LD18:6
LD12:12
LD6:18
**++
LD18:6
**
anterior [AE]
posterior
anterior in LD18:6 [AM]

Figure 3

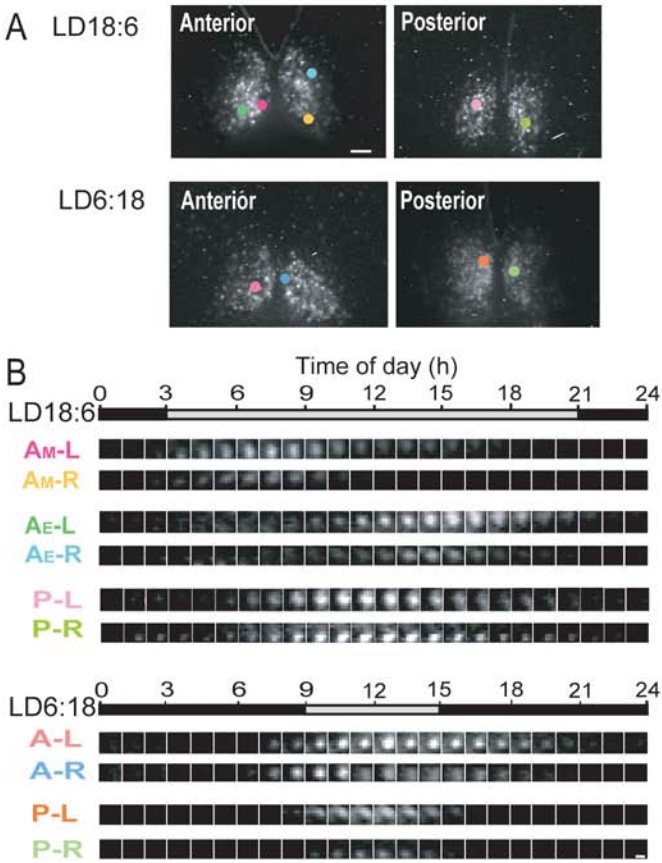
A
LD18:6
Anterior
Posterior
LD6:18
Anterior
Posterior
B
Time of day (h)
0
3
6
9
12
15
18
21
24
LD18:6
AM-L
AM-R
AE-L
AE-R
P-L
P-R
LD6:18
A-L
A-R
P-L
P-R

Figure 4

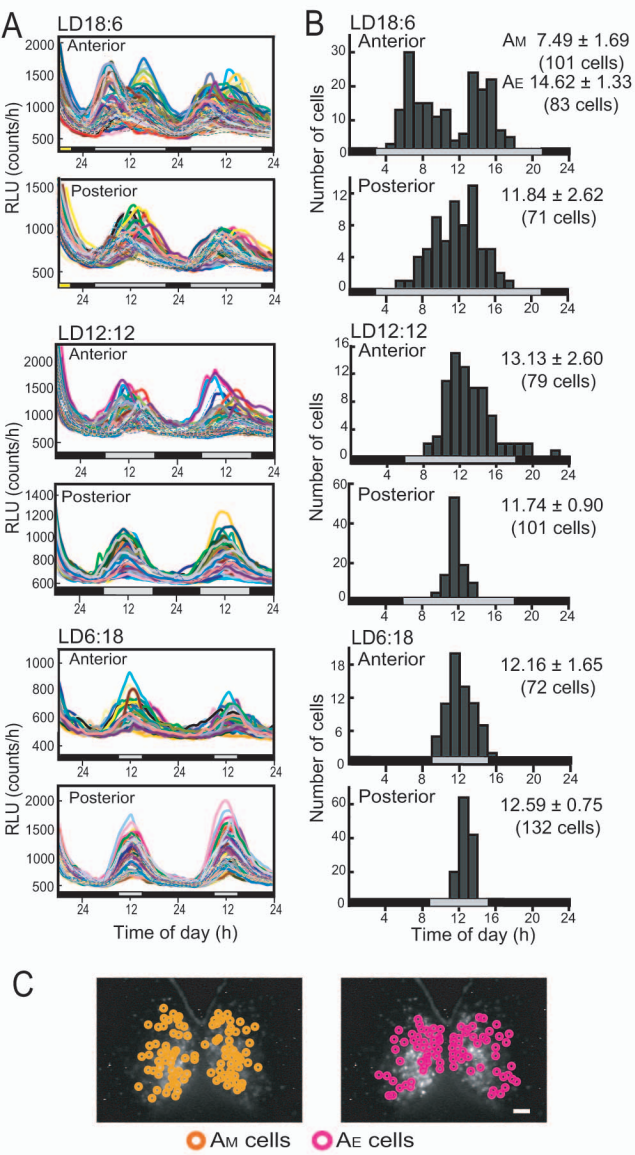
A
LD18:6
Anterior
Posterior
LD12:12
Anterior
Posterior
LD6:18
Anterior
Posterior
RLU (counts/h)
Time of day (h)
B
LD18:6
Anterior
AM 7.49 ± 1.69
(101 cells)
AE 14.62 ± 1.33
(83 cells)
Posterior
11.84 ± 2.62
(71 cells)
LD12:12
Anterior
13.13 ± 2.60
(79 cells)
Posterior
11.74 ± 0.90
(101 cells)
LD6:18
Anterior
12.16 ± 1.65
(72 cells)
Posterior
12.59 ± 0.75
(132 cells)
Number of cells
Time of day (h)

C
AM cells
AE cells

Figure 5

Legend of Supporting Figures

Supporting Fig. 1 Changes in the activity time after mice were released into DD

A, Changes in the length of daily activity band ($\Delta\alpha$) from the averaged length of the last 5 days in LD were calculated for 15 days after released in DD. The value on day 0 indicates the difference between the averaged length and the length on the last day in LD. It took about 14 days for the activity band to be fully decompressed when released from LD18:6, whereas no change was detected when released from LD6:18. **B,** Daily activity times were calculated for 15 days after released in DD from LD 18:6 (closed circles) and from LD6:18 (open circles). The value on day 0 indicates the activity time on the last day in LD. Two way repeated measure ANOVA analysis revealed significant differences ($p<0.01$) in activity time with factors time (days in DD), conditions (LD18:6 vs LD6:18) and time*conditions. Data are mean±SD.

Supporting Fig. 2 Anterior and posterior SCN slices, and distribution of AVP and VIP immunoreactive cells

A, Phase contrast photomicrographs demonstrating the planes of anterior and posterior SCN slices. Broken lines indicate dissected SCN areas for *Per1-luc* activity monitoring. OC, optic chiasm. Scale bar, 100 μ m. **B**, Double-labeling confocal images of VIP (red) and AVP (green) immunoreactivity in the anterior and posterior SCN. Mice were deeply anesthetized and perfused intracardially with 0.1M phosphate-buffered saline followed by 4% paraformaldehyde in 0.1M PB. Fluoro-images of immunoreactive AVP and VIP were visualized by confocal laser scanning microscopy after incubating with anti-mouse goat IgG conjugated with Alexa 488, and anti-rabbit goat IgG with Alexa 594, respectively. Scale bar, 100 μm.

Supporting Fig. 3 Temporal distribution of individual circadian peaks

Temporal distribution of individual circadian *Per1-luc* peaks on day1 of culture in total 3 SCN slices for each phtoperiod. Numbers are the mean and SD. For A_M and A_E groups of the anterior SCN in LD18:6, the average phase was calculated excluding peaks at 11h.

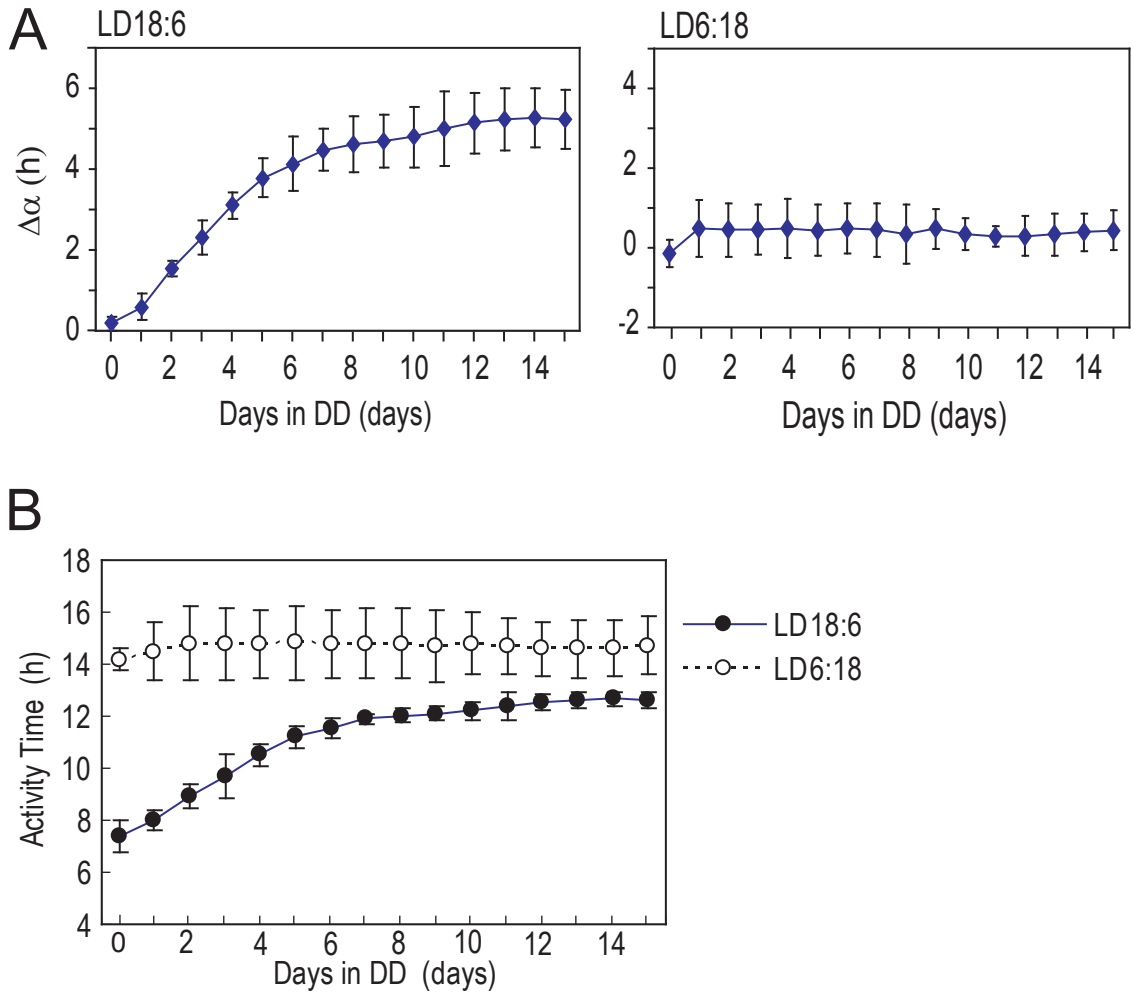
A
LD18:6
LD6:18
Δα (h)
Days in DD (days)
Days in DD (days)
B
Activity Time (h)
Days in DD (days)
LD18:6
LD6:18

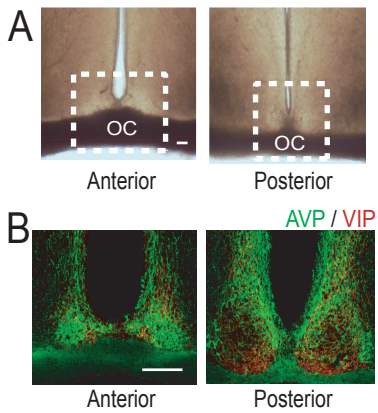
A
OC
OC
Anterior
Posterior
B
AVP / VIP
Anterior
Posterior

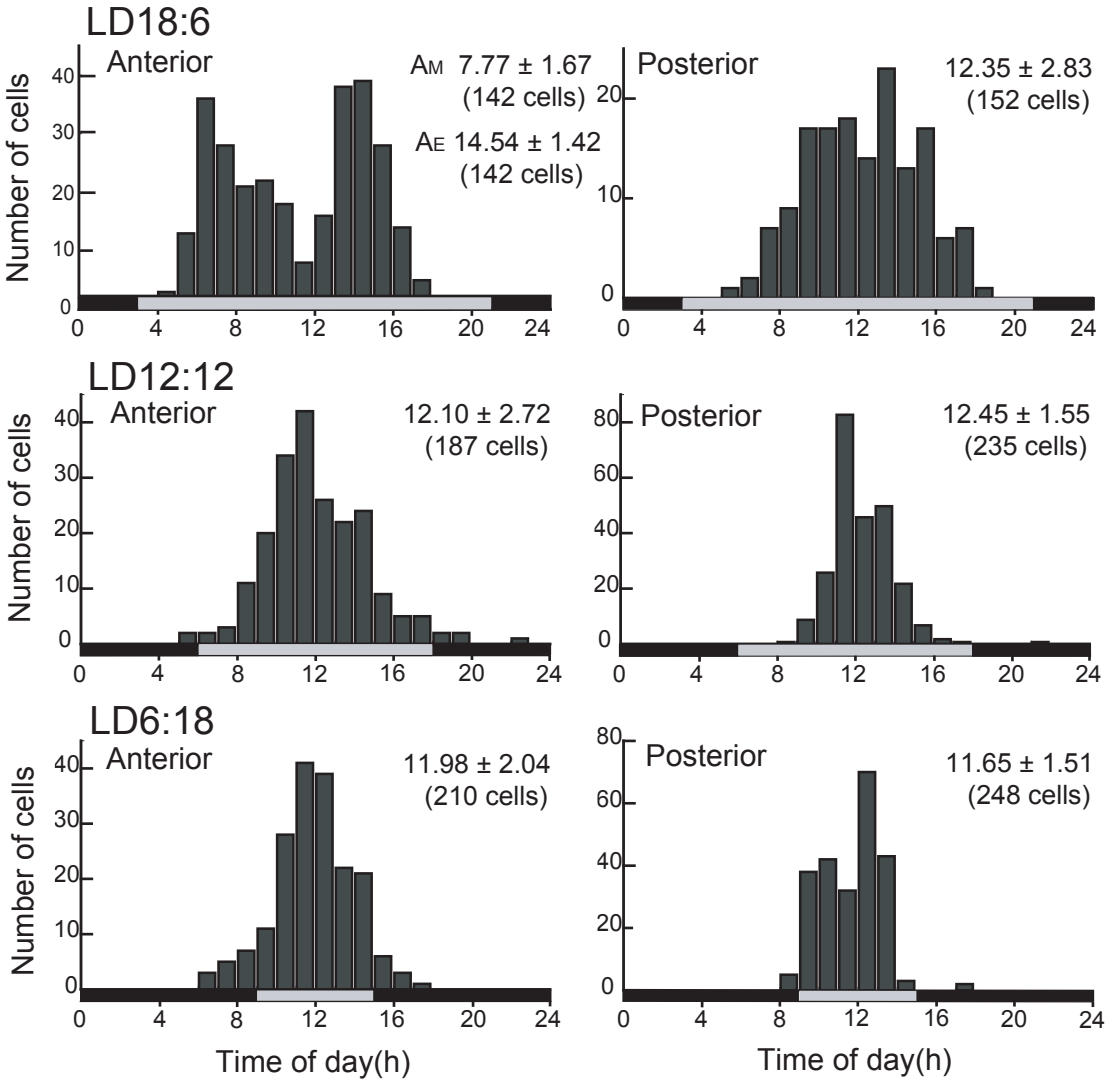
LD18:6
Anterior
AM 7.77 ± 1.67
(142 cells)
AE 14.54 ± 1.42
(142 cells)
Posterior
12.35 ± 2.83
(152 cells)
LD12:12
Anterior
12.10 ± 2.72
(187 cells)
Posterior
12.45 ± 1.55
(235 cells)
LD6:18
Anterior
11.98 ± 2.04
(210 cells)
Posterior
11.65 ± 1.51
(248 cells)
Number of cells
Time of day(h)